Quantum interference in carbon nanotube electron resonators induced by an axial magnetic field

2006 J. Phys.: Condens. Matter 18 2149

(http://iopscience.iop.org/0953-8984/18/7/004)

INSTITUTE OF PHYSICS PUBLISHING JOURNAL OF PHYSICS: CONDENSED MATTER

J. Phys.: Condens. Matter **18** (2006) 2149–2156 doi:10.1088/0953-8984/18/7/004

Quantum interference in carbon nanotube electron resonators induced by an axial magnetic field

Yong Zhang[1,2], **Guili Yu**[1], **Fenglan Hu**[1] **and Jinming Dong**[1]

[1] National Laboratory of Solid State Microstructures and Department of Physics, Nanjing University, Nanjing 210093, People's Republic of China
[2] Department of Applied Physics, Nanjing University of Technology, Nanjing 210009, People's Republic of China

Received 18 October 2005, in final form 3 January 2006
Published 2 February 2006
Online at stacks.iop.org/JPhysCM/18/2149

Abstract

The quantum interference in single-walled carbon nanotubes (SWNTs) in a magnetic field parallel to their axes has been studied analytically. It is found that the quantum conductance changes with magnetic field periodically, which is consistent with the experimental observations. The rapid and slow conductance oscillation periods for both armchair and zigzag SWNTs have been derived analytically; they depend now on both the magnetic field and gate voltage in addition to the sample length. More interestingly, metallic zigzag SWNTs in an axial magnetic field can have slow conductance oscillation, which should not exist without a magnetic field being applied.

(Some figures in this article are in colour only in the electronic version)

Electron transport behaviour in SWNTs is of fundamental and practical interest [1–8]. It was found that a metallic SWNT has a very long mean free path [9], resulting in a long coherence length of the conduction electrons even when there exist a lot of impurities or defects in the nanotube, which permits quantum interference between forward and backward propagating electron waves along the tube axis. Many aspects of these effects have been introduced and studied previously [4–13]. It was reported that electron interference in a perfect-contacted SWNT is manifest as conductance oscillations versus Fermi energy with the oscillation period determined by the nanotube length [10, 11]. Observation of two units of quantum conductance $4e^2/h$ indicates the ballistic motion of electrons in the nanotubes. A rapid conductance oscillation superimposed on a slow one was also observed and ascribed to the possible disorder effect in the nanotube [10, 11]. However, Jiang *et al* showed [12] analytically that both the rapid and slow conductance oscillations are caused by the intrinsic quantum interference. Yang *et al*'s numerical results [13] support the analytical conclusions.

On the other hand, theoretical analysis showed that an axial magnetic field, and thus Aharonov–Bohm (AB) flux Φ, can change the electronic and transport properties of a given nanotube [14–19]. The AB effect is caused by the interference between the electron waves

encircling the nanotube in two opposite directions [17–19]. When threaded by a magnetic flux Φ, the band structure of a nanotube was predicted to depend on Φ/Φ_0, making the band gap oscillate with a period Φ_0, where Φ_0 $(=h/e)$ is the fundamental magnetic flux quantum. Recently, an experimental measurement on the quantum conductance in a multiwalled carbon nanotube (MWNT) [18] in an axial magnetic field was reported, in which a periodical change of conductance with magnetic field was found. Another experiment on the magnetoresistance measurement on an individual MWNT [19] also showed that the resistance oscillates as a function of magnetic flux Φ. However, there are no experimental and theoretical researches up to now of the magnetic field effect on quantum interference in carbon nanotubes.

In this paper we will discuss the quantum conductance oscillations in MWNT resonators in an axial magnetic field, which could be simulated by a large diameter SWNT because the transport properties of an MWNT can usually be considered only to be determined by its outermost tube [18, 19]. The quantum conductance is found to change with magnetic field periodically, which is consistent with the experimental results [18, 19]. Specifically, the variations of both rapid and slow conductance oscillation periods with magnetic field for armchair and metallic zigzag SWNTs are derived analytically. More interestingly, a slow conductance oscillation is found to exist in the metallic zigzag SWNTs in an axial magnetic field, which should not be found in them if no magnetic field is applied.

An SWNT can be defined by a two-dimensional (2D) lattice vector $\vec{R} = n_1\vec{a}_1 + n_2\vec{a}_2$ with $\vec{a}_1, \vec{a}_2$ ($|\vec{a}_1| = |\vec{a}_2| = a$) the 2D unit vectors of a graphite sheet and n_1, n_2 integers. The SWNTs with $n_1 - n_2 = 3k$ (k an integer) are metallic, and the others are semiconductors. The SWNT is characterized by rotation and screw operation. Based upon these symmetries, we can define its unit cell with the unit vectors $\vec{b}_1 = \vec{H}$ and $\vec{b}_2 = \vec{R}/N$. Here, $\vec{H} = p_1\vec{a}_1 + p_2\vec{a}_2$ with $p_1 \geqslant 0$ and the pair of integers p_1 and p_2 satisfy the condition $n_2 p_1 - n_1 p_2 = N$ with N the largest common divisor of n_1 and n_2. A unit cell in the SWNT can be labelled by (m, l) with m and l the number of applications of screw and rotation operation, respectively. The reciprocal lattice unit vectors $\vec{k}_1$ and $\vec{k}_2$ corresponding to the real space vectors $\vec{b}_1$ and $\vec{b}_2$ are given, respectively, by

$$\begin{aligned} \vec{k}_1 &= \frac{2(2n_2 + n_1)}{3Na^2}\vec{a}_1 - \frac{2(2n_1 + n_2)}{3Na^2}\vec{a}_2 \\ \vec{k}_2 &= -\frac{4\pi(2p_2 + p_1)}{3a^2}\vec{a}_1 + \frac{4\pi(2p_1 + p_2)}{3a^2}\vec{a}_2. \end{aligned} \tag{1}$$

Here $\vec{k}_1$ has been divided by 2π. The wavevector for the SWNT can be introduced by $\vec{k} = k\vec{k}_1 + (\nu/N)\vec{k}_2$, with $-\pi \leqslant k \leqslant \pi$ and $\nu = 0, 1, \ldots, N-1$. The allowed $\vec{k}$ values for an SWNT lie on parallel lines with a spacing of $2\pi/|\vec{R}|$.

In a uniform magnetic field parallel to the tubular axis, the allowed electron states can be expressed as

$$\vec{k} = k\vec{k}_1 + (\nu/N)\vec{k}_2 - (\mathrm{e}/c\hbar)\vec{A}. \tag{2}$$

By choosing $\vec{A} = -\vec{B} \times \vec{r}/2$, we obtain $\vec{k} \cdot \vec{R} = 2\pi\eta + 2\pi\phi/\phi_0$ with η an integer, which indicates that the magnetic field moves the parallel lines (allowed electron states) by a distance of $(2\pi/|\vec{R}|)(\phi/\phi_0)$ along $\vec{R}$. So, metallic SWNTs remain metallic at $\phi = J\phi_0$ (J an integer), but the semiconducting SWNTs can become metallic for $\phi = (J \pm \frac{1}{3})\phi_0$ [15].

So, near the Fermi surface, the energy dispersion relation for the armchair SWNT in an axial magnetic field can be expressed as

$$E_k^{\pm} = \pm\gamma\sqrt{4\cos^2\left(k - \frac{J\pi}{N}\right) + 4\cos\left(k - \frac{J\pi}{N}\right)\cos\frac{p\pi}{N} + 1}, \tag{3}$$

where $\phi/\phi_0 = J + p$ with J an integer, and p is a fraction. If $J = 0$, $0 \leqslant p \leqslant 1/2$, else $-1/2 \leqslant p \leqslant 1/2$.

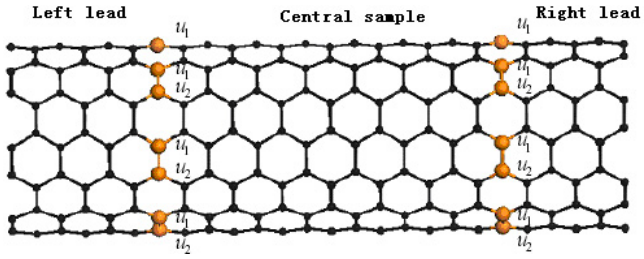

Figure 1. A schematic diagram of an armchair nanotube electron resonator. The atoms on a highlighted ring construct an interface.

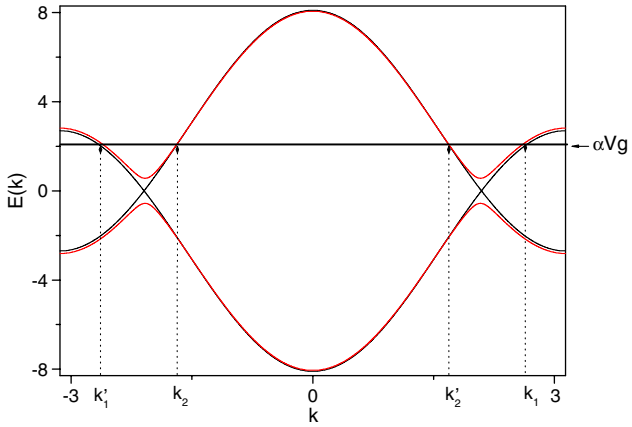

Figure 2. Energy bands of the armchair nanotube near the Fermi level in an axial magnetic field, where the black and grey curves correspond to $\Phi/\Phi_0 = 0$ and 0.4, respectively.

A Fabry–Perot electron resonator based on an armchair SWNT is shown schematically in figure 1. The whole model system consists of a central sample with a finite length and two semi-infinite leads (left and right), which are assumed to be made of the same kind of SWNT. Each interface between a lead and the sample is represented by a ring of atoms, which may be regarded as a kind of defect. We introduce on-site energies of u_1, u_2 to model the barrier potential at the interface [12].

For a given energy, there are four degenerate states in the energy bands of an armchair SWNT, and their wavevectors are k_1, k_1', k_2 and k_2' (see figure 2) with a relation of $k_1' = -k_1 + \frac{2J\pi}{N}$ and $k_2' = -k_2 + \frac{2J\pi}{N}$, where k_1 and k_2 represent the states near $k_{1\mathrm{F}} = \frac{J\pi}{N} + \arccos[-\frac{1}{2}\cos(\frac{p\pi}{N})]$ and $k_{2\mathrm{F}} = \frac{J\pi}{N} - \arccos[-\frac{1}{2}\cos(\frac{p\pi}{N})]$, respectively. Under the tight-binding approximation, the wavefunctions of the four degenerate states are given by

$$\begin{aligned}\psi_{k_j} &= \frac{1}{\sqrt{2MN}}\sum_{m=0}^{M-1}\sum_{l=0}^{N-1} \mathrm{e}^{\mathrm{i}k_j m}(|ml;1\rangle \pm \mathrm{e}^{\mathrm{i}\varphi}|ml;2\rangle)\\ \psi_{k_j'} &= \frac{1}{\sqrt{2MN}}\sum_{m=0}^{M-1}\sum_{l=0}^{N-1} \mathrm{e}^{\mathrm{i}k_j' m}(|ml;1\rangle \pm \mathrm{e}^{\mathrm{i}\varphi}|ml;2\rangle).\end{aligned} \tag{4}$$

Here, the + sign stands for $j = 1$ and the − sign for $j = 2$; $|ml;1\rangle$ ($|ml;2\rangle$) denotes the $|p_\perp\rangle$ orbital of the carbon atom labelled as 1 (2) in a unit cell of the SWNT, φ is their phase difference and M is the total number of applications of screw operation.

At the zero-temperature and zero-bias limit, the incident and outgoing electrons are set to have Fermi energy, so their wavevectors are Fermi vectors $k_{1\mathrm{F}}$ and $k_{2\mathrm{F}}$, respectively. In the SWNT resonator, their kinetic energy can be changed by the gate voltage V_g, which introduces a potential energy of $-\alpha V_\mathrm{g}$ with α the gate efficiency factor. So, by using equation (3), the

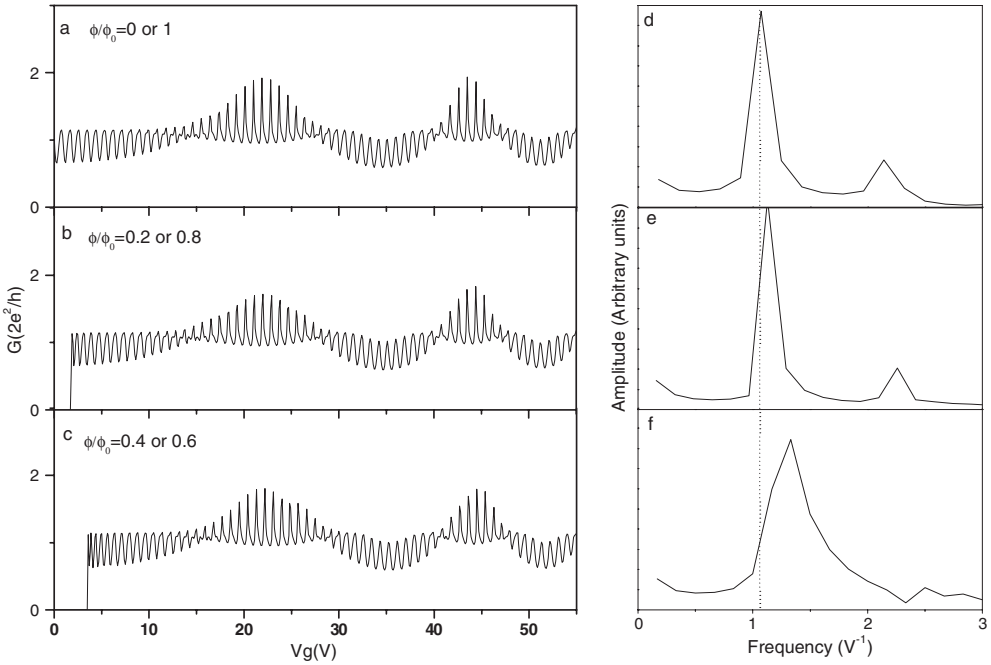

Figure 3. Left panel: conductance G versus V_g for the (96, 96) armchair nanotube in an axial magnetic field with $\alpha = 0.01$, $u_1 = 1.0$ eV, $u_2 = 6.0$ eV, and $M = 1624$. (a)–(c) correspond to $\Phi/\Phi_0 = 0$ (or 1), 0.2 (or 0.8), and 0.4 (or 0.6), respectively. Right panel: the Fourier frequency analysis of the rapid conductance oscillations for the (96, 96) armchair nanotube at the gate voltage of near 22 eV, where the curves in (d)–(f) correspond to those of (a)–(c), respectively.

wavevectors of k_1 and k_2 (figure 2) in the resonator are determined by

$$-\alpha V_g = \pm\gamma\sqrt{4\cos^2\left(k_1 - \frac{J\pi}{N}\right) + 4\cos\left(k_1 - \frac{J\pi}{N}\right)\cos\frac{p\pi}{N} + 1}$$

for $k > k_{1F}$

$$-\alpha V_g = \pm\gamma\sqrt{4\cos^2\left(k_2 - \frac{J\pi}{N}\right) + 4\cos\left(k_2 - \frac{J\pi}{N}\right)\cos\frac{p\pi}{N} + 1} \tag{5}$$

for $0 > k > k_{2F}$

where $\gamma = -2.7$ eV is the nearest-neighbour hopping amplitude [20]. With the help of equation (4), the boundary conditions are constructed through the continuity equations [1, 2] and the equation of motion [21] at the sites on the boundary. Then, one can analytically derive the transmission coefficient $t_{il,jr}$ for a wave going from the ith channel on the left electrode to the jth channel on the right electrode, from which the quantum conductance[3] of the electron resonator can be given out using Landauer–Büttiker formula [22–24]

$$G = (2e^2/h)\sum_{i,j=1}^{2}\left|t_{ij}\right|^2. \tag{6}$$

Figures 3(a), (b) and (c) give three plots of the conductance of a (96, 96) armchair SWNT versus gate voltage (G–V_g) with $u_1 \neq u_2$, in which $u_1 = 1.0$ eV, $u_2 = 6.0$ eV and $\phi/\phi_0 = 0$

[3] The expressions of $t_{il,jr}$ are too tedious to be given out here.

(or 1), 0.2 (or 0.8) and 0.4 (or 0.6), respectively. Here, M is taken as 1624, corresponding to a nanotube length of about 200 nm. The parameter α is taken to be 0.01, estimated from the capacitance of a nanotube in [12, 13]. It can be seen obviously from figure 3 that the conductance changes with magnetic field (ϕ/ϕ_0) periodically with a period of ϕ_0.

It should be pointed out that the SWNTs are ultra-small with a typical radius of ∼1 nm, for which the magnetic field needed to get $1\phi_0$ flux through their cross sections should be $B \sim 1000$ T, far beyond the limit of available experimental magnetic fields. Recently, an experiment [18] on the quantum conductance of an MWNT threaded by an axial magnetic field was reported, in which it was found that only the outermost shell of the MWNT contributes to the conduction, and the interaction from other inner walls is weak and can be neglected. The outmost shell of the MWNT used in this experiment has a radius of $r \approx 15$ nm, for which a magnetic field of $B \approx 5.8$ T can induce $1\phi_0$ magnetic flux. Another experimental measurement [19] on the magnetoresistance of an MWNT shows an oscillating resistance as a function of magnetic field B with a period of 17.6 T, from which a radius $r = 8.6$ nm of the outmost wall was inferred and proved by atomic-force microscopy. So, in figure 3, we take a large radius SWNT (96, 96) with its $r \approx 6.5$ nm to model the MWNT, and a periodical change of the quantum conductance with magnetic field is also found with a period of $1\phi_0$ (31 T). Our analytical conclusion is consistent with the experimental result [18, 19] even though it is derived from an SWNT with its radius compatible with that of the outermost shell in the MWNT.

As mentioned above, the conduction electrons in the SWNTs have a very long coherence length (up to micrometre size), while the transmitted electron waves (k_1, k_2) in the nanotubes can be reflected by the electrodes (see figure 1) one after another, inducing an interference between the same electron waves (k_1 or k_2, which is the origin of rapid conductance oscillation) and different ones (k_1 and k_2, which is the origin of slow conductance oscillation) [25]. Our model system is just like a Fabry–Perot resonator. So in [12], the rapid and slow conductance oscillations are interpreted to be an intrinsic quantum interference phenomenon, and are ascribed to the contributions from the linear and nonlinear terms, respectively, of the energy dispersion relations. Following the method in [12], we can also find analytically the rapid and slow conductance oscillation periods for an armchair nanotube at $\phi/\phi_0 = J + p$, which can be approximately expressed as

$$\begin{aligned} \Delta V_{\mathrm{g}}^{\mathrm{r}} &= \frac{\sqrt{3}\pi\,|\gamma|}{\alpha M}\sqrt{1-\left(\frac{p\frac{\gamma\pi}{N}}{\alpha V_{\mathrm{g}}}\right)^2} \\ \Delta V_{\mathrm{g}}^{\mathrm{s}} &= \frac{\sqrt{3}\,|\gamma|}{\alpha}\left(\frac{2\sqrt{3}\pi}{M}\right)^{1/2}\sqrt{1-\left(\frac{p\frac{\gamma\pi}{N}}{\alpha V_{\mathrm{g}}}\right)^2}\,(\sqrt{n}-\sqrt{n-1}). \end{aligned} \tag{7}$$

Here, $|\alpha V_{\mathrm{g}}| \geqslant |p\frac{\gamma\pi}{N}|$ with $2|p\frac{\gamma\pi}{N}|$ being the band gap of an armchair SWNT induced by the axial magnetic field [15]. It is clearly seen from equation (7) that the rapid and slow oscillation periods change periodically with the magnetic flux, and both of them decrease with $|p|$ in the same form of $\sqrt{1-\left((p\frac{\gamma\pi}{N})/(\alpha V_{\mathrm{g}})\right)^2}$. So, the rapid and slow oscillations become faster for $0 < p < 1/2$ and slower for $-1/2 < p < 0$ with increasing magnetic field, which is also illustrated by the Fourier frequency analysis shown in the right-hand panel of figure 3. The rapid oscillation becomes especially severe near the band gap (i.e., $\alpha V_{\mathrm{g}} \approx p\frac{\gamma\pi}{N}$) because now the factor of $(p\frac{\gamma\pi}{N})/(\alpha V_{\mathrm{g}})$ is approaching 1. At a fixed magnetic field, both $\Delta V_{\mathrm{g}}^{\mathrm{r}}$ and $\Delta V_{\mathrm{g}}^{\mathrm{s}}$ would increase with increasing V_{g}.

On the other hand, from equation (7), we can find that, although both the rapid and slow conductance oscillation periods depend on magnetic field, gate voltage, efficiency factor and sample length, their ratio is dependent only on the sample length, which is identical as in the

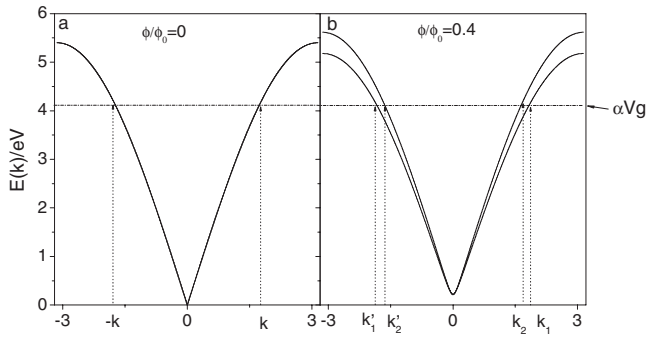

Figure 4. Energy bands of a metallic (27, 0) zigzag nanotube near the Fermi level in an axial magnetic field. (a) $\Phi/\Phi_0 = 0$, and (b) $\Phi/\Phi_0 = 0.4$.

case of no magnetic field [12]. So for any experiments with different magnetic fields, gate voltages and gate efficiencies, but the same tube length, there will still be the same number of rapid oscillation periods within a slow oscillation period.

At large enough gate voltages, e.g., $|\alpha V_g| \gg |p\frac{\gamma\pi}{N}|$, the rapid and slow oscillation periods can be approximately expressed as

$$\begin{aligned} \Delta V_g^r &= \Delta V_g^{r0}\left[1 - \frac{1}{2}\left(\frac{p\frac{\gamma\pi}{N}}{\alpha V_g}\right)^2\right] \\ \Delta V_g^s &= \Delta V_g^{s0}\left[1 - \frac{1}{2}\left(\frac{p\frac{\gamma\pi}{N}}{\alpha V_g}\right)^2\right], \end{aligned} \tag{8}$$

where ΔV_g^{r0} and ΔV_g^{s0} are their periods without magnetic field [12]. It is apparent that the influence of magnetic field on the rapid and slow conductance periods becomes weaker when far away from the band gap.

It is convenient to estimate the rapid and slow oscillation periods using equation (8). For example, for the (96, 96) SWNT with $M = 1624$, $p = 0.2$ and $\alpha = 0.01$, if V_g is taken to be about 22 eV, we can get a rapid oscillation period of $\Delta V_g^r \approx 0.8903$ V, and so its frequency is 1.13 V^{-1}, which is consistent with that of the Frouier frequency analysis shown in figure 3(e).

Now, we discuss the case of metallic zigzag SWNTs, which have two degenerate subbands near the Fermi surface in the case of no magnetic field (see figure 4(a)), $E_k^{\pm} = \pm 2\gamma \sin(\frac{k}{2})$, making the phase difference between the two modes to remain constant, and so no slow conductance oscillation is found in them [12] (see figure 5(a)). However, in an axial magnetic field, the band degeneracy is lifted (see figure 4(b)), and the energy dispersions of the two degenerate bands become

$$E_k^{\pm} = \pm\gamma\sqrt{4\cos\left(k - \frac{3J\pi}{N}\right)\cos\left(\frac{2\pi}{3} + \frac{p\pi}{N}\right) + 4\cos^2\left(\frac{\pi}{3} - \frac{p\pi}{N}\right) + 1} \tag{9a}$$

and

$$E_k^{\pm} = \pm\gamma\sqrt{4\cos\left(k - \frac{3J\pi}{N}\right)\cos\left(\frac{2\pi}{3} - \frac{p\pi}{N}\right) + 4\cos^2\left(\frac{\pi}{3} + \frac{p\pi}{N}\right) + 1} \tag{9b}$$

respectively, making the two modes to have a phase difference now, and so the metallic zigzag SWNTs can also have both rapid and slow conductance oscillations in an axial magnetic field (see figures 5(b) and (c)).

With the help of equations (9*a*) and (9*b*), the rapid and slow quantum conductance oscillation periods of metallic zigzag SWNTs in an axial magnetic field can be obtained as

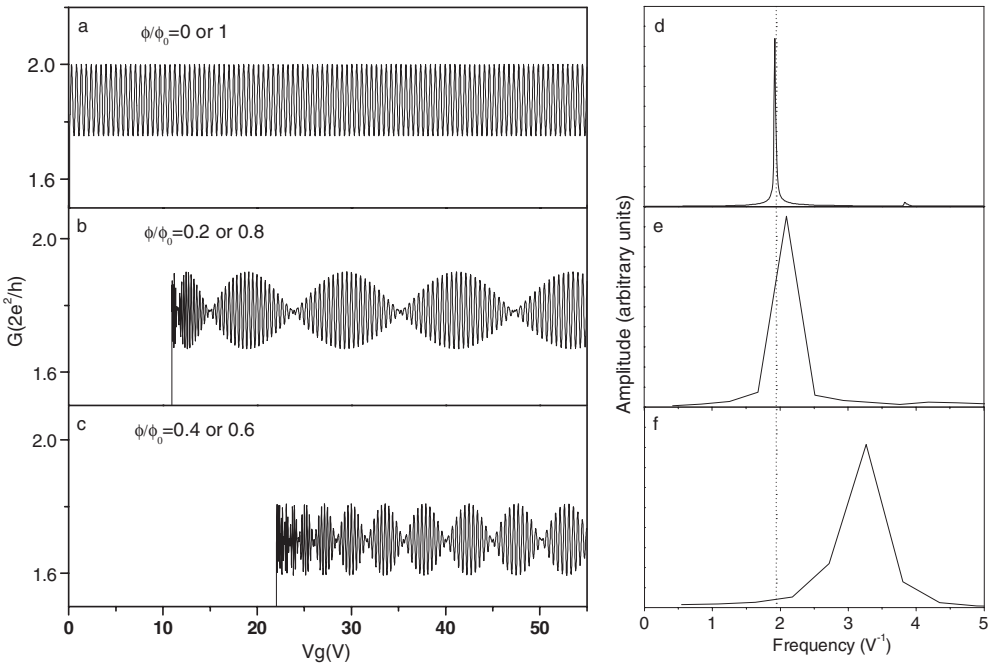

Figure 5. The same plots as figure 3 but for the zigzag nanotube (27, 0). Right panel: the Fourier frequency analysis of the rapid conductance oscillations taken at a gate voltage of about 27 eV.

follows:

$$\Delta V_{\mathrm{g}}^{\mathrm{r}} = \frac{\pi\,|\gamma|}{\alpha M}\sqrt{1-\left(\frac{p\frac{\sqrt{3}\pi\gamma}{N}}{\alpha V_{\mathrm{g}}}\right)^2}$$
$$\Delta V_{\mathrm{g}}^{\mathrm{s}} = \frac{2N\,|\gamma|}{\sqrt{3}M\,|p|\,\alpha}\sqrt{1-\left(\frac{p\frac{\sqrt{3}\pi\gamma}{N}}{\alpha V_{\mathrm{g}}}\right)^2}. \tag{10}$$

From equation (10), it is clearly seen that, at a certain magnetic field, the rapid and slow oscillations become faster near the band gap (i.e., $\alpha V_{\mathrm{g}} \approx p\frac{\sqrt{3}\pi\gamma}{N}$), and slower with increasing V_{g}. The rapid conductance oscillation period decreases with increasing magnetic field for $0 < p < 1/2$, while it increases with increasing magnetic field for $-1/2 < p < 0$, which also could be found from the Fourier frequency analysis shown in the right-hand panel of figure 5.

If $|\alpha V_{\mathrm{g}}| \gg |p\frac{\sqrt{3}\pi\gamma}{N}|$, $p\frac{\sqrt{3}\pi\gamma}{N}/\alpha V_{\mathrm{g}} \approx 0$, the rapid and slow oscillation periods can be simplified as

$$\Delta V_{\mathrm{g}}^{\mathrm{r}} = \frac{\pi\,|\gamma|}{\alpha M}$$
$$\Delta V_{\mathrm{g}}^{\mathrm{s}} = \frac{2N\,|\gamma|}{\sqrt{3}M\,|p|\,\alpha}. \tag{11}$$

From equation (11), it is apparent that far away from the band gap, the rapid conductance oscillation period is independent of magnetic field (p) and gate voltage (V_{g}), while the slow conductance oscillation period is proportional to $1/|p|$ (see figures 5(b) and (c)). If $p = 0$, the $\Delta V_{\mathrm{g}}^{\mathrm{s}} \to \infty$, recovering again that of [12] (see figure 5(a)).

Finally, we should point out that the rapid and slow oscillation periods of carbon nanotubes given in [12] are dependent on only the nanotube length and do not change with the gate voltage V_g. However, in an axial magnetic field, they are dependent on both the nanotube length and the gate voltage V_g. From this point of view, they are not a 'true' periodical oscillation, and they change with V_g successively. It is seen from our analytical expressions for the rapid and slow oscillation periods and the Fourier frequency analysis of them that for a certain range of V_g, they can still be approximately considered as a kind of oscillation with well-defined period described conveniently by our analytical formula.

In conclusion, we have discussed quantum interference in carbon nanotubes in an axial magnetic field, and derived analytically the rapid and slow conductance oscillation periods for armchair and metallic zigzag SWNTs. It is found that the quantum conductance changes with magnetic field periodically, which is consistent with the experimental observations. Both the rapid and slow conductance oscillation periods also change periodically with the magnetic flux. In addition, we have found that the slow conductance oscillation can also exist in metallic zigzag SWNTs, which was not found in them without a magnetic field being applied.

Acknowledgments

This work was supported by the Natural Science Foundation of China under Grant Nos 10474035, 90503012, and also by the State Key Program of China through Grant No 2004CB619004.

References

[1] Ando T *et al* 1998 *Mesoscopic Physics and Electronics* (Berlin: Springer)
[2] Datta S 1995 *Electronic Transport in Mesoscopic Systems* (Cambridge: Cambridge University Press)
[3] Van Wees B J *et al* 1989 *Phys. Rev. Lett.* **62** 2523
[4] Crommie M F *et al* 1993 *Science* **262** 218
[5] Ji Y *et al* 2000 *Science* **290** 779
[6] Topinka M A *et al* 2000 *Science* **289** 2323
[7] Manoharan H C *et al* 2000 *Nature* **403** 512
[8] Debray P *et al* 2000 *Phys. Rev.* B **61** 10950
[9] Tans S J *et al* 1997 *Nature* **386** 474
[10] Liang W *et al* 2001 *Nature* **411** 665
[11] Kong J *et al* 2001 *Phys. Rev. Lett.* **87** 106801
[12] Jiang J *et al* 2003 *Phys. Rev. Lett.* **91** 056802
[13] Yang L *et al* 2004 *Phys. Rev.* B **69** 153407
[14] Ajiki H *et al* 1993 *J. Phys. Soc. Japan* **62** 1255
[15] Jiang J *et al* 2000 *Phys. Rev.* B **62** 13209
[16] Lin M F *et al* 1995 *Phys. Rev.* B **51** 7592
[17] Cao J *et al* 2004 *Phys. Rev. Lett.* **93** 216803
[18] Coskun T C *et al* 2004 *Science* **304** 1132
[19] Bachtold A *et al* 1999 *Nature* **397** 673
[20] White C T *et al* 1993 *Phys. Rev.* B **47** 5485
[21] Matsumura H *et al* 1998 *J. Phys. Soc. Japan* **67** 3542
[22] Büttiker M *et al* 1985 *Phys. Rev.* B **31** 6207
[23] Büttiker M 1986 *Phys. Rev.* B **33** 3020
[24] Cahay M *et al* 1988 *Phys. Rev.* B **37** 10125
[25] White C T *et al* 2001 *Nature* **411** 649